PHYSICAL REVIEW B **74**, 041306(R) (2006)

Intrinsic ferromagnetism in wurtzite (Ga,Mn)N semiconductor

E. Sarigiannidou,[1,*] F. Wilhelm,[2] E. Monroy,[1] R. M. Galera,[3] E. Bellet-Amalric,[1] A. Rogalev,[2] J. Goulon,[2] J. Cibert,[3] and H. Mariette[1]

[1]*CEA-CNRS-UJF group "Nanophysique et Semiconducteurs," DRFMC/SP2M/PSC, CEA-Grenoble, 17 rue des Martyrs, 38054 Grenoble Cedex 9, France*

[2]*European Synchrotron Radiation Facility (ESRF), Boíte Postale 220, 38043 Grenoble, France*

[3]*Laboratoire Louis Néel, CNRS, Boíte Postale 166, 38042 Grenoble, France*

(Received 14 March 2006; revised manuscript received 15 June 2006; published 19 July 2006)

Intrinsic ferromagnetism in the high-quality wurtzite $Ga_{0.937}Mn_{0.063}N$ semiconductor is unambiguously demonstrated by both macroscopic magnetization measurements and x-ray magnetic circular dichroism. The structural quality of the samples grown by plasma-assisted molecular beam epitaxy is confirmed by x-ray diffraction and x-ray linear dichroism. The Curie temperature of a (Ga,Mn)N sample with 6.3% Mn is ≈8 K with a spontaneous magnetic moment of $2.4\mu_B$ per Mn at 2 K.

DOI: 10.1103/PhysRevB.74.041306 PACS number(s): 75.50.Pp, 75.70.Ak, 78.70.Dm, 81.15.Hi

The pioneering work of Dietl *et al.*[1] has impelled worldwide research on wide bandgap diluted magnetic semiconductors (DMSs) due to the prediction of ferromagnetism above room temperature for materials such (Ga,Mn)N, (Zn,Mn)O, and Mn-doped diamond. In the case of (Ga,Mn)N, many laboratories have succeeded in the growth of thin layers, although their electronic and magnetic properties remain under debate.[2–4] Some reports on wurtzite (Ga,Mn)N films present a ferromagneticlike state with a T_C which varies from liquid helium temperature[5] up to 940 K,[6] whereas in zinc-blende (Ga,Mn)N films a ferromagnetic correlation has been observed only at low temperatures.[7] In parallel, recent *ab initio* calculations[8] predict a low T_C.[9] The observation of a ferromagneticlike state at high temperatures could therefore be related to structural defects, such as inclusions of Mn_4N (T_C=784 K),[10] $Mn_{3-\delta}Ga$ (T_C=765 K),[11] or $Mn_{3.2}Ga_{0.8}N$ (T_C=235 K).[12] Therefore, single-phase (Ga,Mn)N layers are required to clarify the electronic and magnetic properties of Mn atoms, and consequently to understand the origin of ferromagnetism in this DMS. Once the structural quality of the layers is confirmed, highly sensitive characterization techniques exploiting the polarization of synchrotron radiation [x-ray linear dichroism (XLD) and x-ray magnetic circular dichroism[13] (XMCD)] are adequate procedures, complementary to standard characterization techniques (e.g. x-ray diffraction and magneto-optical and magnetotransport techniques), to reveal the structural, electronic, and magnetic properties of any DMS material. To the best of our knowledge, among the III-V DMSs, only (Ga,Mn)As, (In,Mn)As, and (Ga,Mn)P have been shown to exhibit ferromagnetism by XMCD.[14–17] A ferromagnetic ordering above room temperature has been observed in (Ga,Mn)N using soft x-ray XMCD, and has been assigned to the presence of structural defects.[3]

In this Rapid Communication, we present a thorough study of the structural, electronic, and magnetic properties of (Ga,Mn)N films grown by molecular beam epitaxy. Experiments based on polarized x rays (XLD and XMCD) are used to clarify the nature of the ferromagnetism.

(Ga,Mn)N layers have been grown using plasma-assisted molecular beam epitaxy (PAMBE), with standard effusion cells for Ga and Mn, and a radio-frequency plasma cell to supply active nitrogen. We have used 10-μm-thick GaN-on-sapphire substrates. The temperature of the substrate was fixed at 715 °C.

We have previously shown that the incorporation of Mn in wurtzite GaN is strongly affected by the Ga:N flux ratio.[18] In this work, special care was taken to optimize the Mn flux as well as the Ga:N ratio in order to maximize Mn incorporation while controlling the two-dimensional growth mode and eliminating the appearance of secondary phases. We have observed for Mn fluxes higher than 4.5×10^{-8} Torr an accumulation of Mn on the (Ga,Mn)N growing surface which is apparently independent of the Ga:N ratio. This Mn accumulation might lead to formation of secondary phases in the layer. On the contrary, below this threshold, incorporation of Mn in the wurtzite structure depends on the Ga:N ratio. For Ga fluxes higher than the stoichiometric value (Ga:N>1), Mn tends to segregate at the growing surface and does not incorporate into the lattice. This situation is illustrated by the reflection high-energy electron diffraction (RHEED) pattern shown in Fig. 1(a), where reflection spots characteristic of the Mn ordering are clearly seen. In the case of heavily N-rich conditions (Ga:N<0.90), Mn is substitutionally incorporated into the wurtzite lattice, but the surface morphology becomes rough, as reflected by a spotty RHEED pattern [Fig. 1(c)]. In between these two extremes an intermediate regime is observed, with Mn being homogeneously incorporated without any significant degradation of the surface morphology of GaN, as one can see on the RHEED pattern [Fig. 1(b)]. We assume that these are the optimal growth conditions of (Ga,Mn)N films. In order to increase the Mn concentration in the samples, we chose a Mn flux close to the

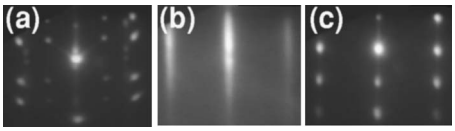

FIG. 1. RHEED patterns in the $\langle 11\bar{2}0\rangle$ azimuth for (a) Mn accumulation on the surface, (b) optimal growth conditions, and (c) extremely N-rich conditions, all with the same Mn flux.

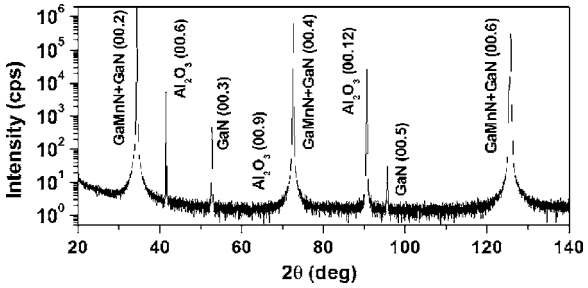

FIG. 2. X-ray diffraction 2θ-θ scan of a (Ga,Mn)N epilayer with 6.3% Mn.

accumulation threshold, and we interrupt periodically the growth process in order to allow the Mn excess to be desorbed from the growing surface. Following this procedure, we have obtained a series of 400-nm-thick single-phase (Ga,Mn)N epilayers with a high amount of Mn atoms. Secondary-ion mass spectroscopy measurements revealed a homogeneous distribution of the Mn across the layer for all Mn concentrations up to $(6.3\pm0.2)\%$, a sample on which we will focus our structural and magnetic study.

The crystalline properties were first investigated by x-ray diffraction using a SEIFERD 3003 PTS diffractometer. The measurements were performed with a beam concentrator prior to a Ge(220) double-bounce monochromator and solar slits in front of the detector, which ensures a dynamic range of 10^6. With this setup, the sensitivity limit to detect secondary phases is estimated to be less than 2% of the sample volume,[19] provided that they present preferential diffraction planes. As illustrated in Fig. 2, no secondary phases are observed in the 2θ-θ scan of samples with 6.3% Mn.

In order to elucidate the site distribution of Mn atoms in the sample and their local symmetry we have used XLD in absorption. XLD is defined as the difference between the x-ray absorption spectra recorded for two orthogonal linear polarization vectors of the x-ray beam.[20] As a differential spectroscopy, it is more sensitive than the isotropic x-ray absorption spectra to small structural distortions or to the presence of secondary phases. We have performed our XLD experiments at the ESRF ID12 beamline.[21] We have exploited a 0.9-mm-thick diamond $\langle 111\rangle$ quarter-wave plate that convert circularly polarized monochromatic x rays into linearly polarized ones.[22] The linear polarization was flipped (1 Hz) from vertical to horizontal at each energy point, while keeping the sample position and the detection solid angle fixed. This setup offers the advantage of a constant footprint of the x-ray beam on the sample.

XLD spectra were recorded at the K edge of both Ga and Mn in (Ga,Mn)N using total fluorescence yield detection mode. The main advantage of performing experiments at the K edges is that one probes the bulk properties and not only the surface layer as is the case for experiments at the L edges. The incidence angle of the x-ray beam on the sample was 10°. For this experimental configuration, the XLD spectra reflect directly the anisotropy in the (a,c) plane of the unoccupied density of states of the $4p$ shell of the Ga and Mn atoms. Figure 3 shows x-ray absorption near-edge structure (XANES) spectra recorded for two orthogonal polarizations, and their difference (XLD), at the Mn and Ga K edges for (Ga,Mn)N with 6.3% Mn. The Ga K-edge XANES spectra are nicely structured with a maximum XLD signal of the order of 58% with respect to the edge jump. The XLD spectra are, within experimental uncertainties ($<0.01\%$), identical to the spectra measured on a monocrystalline wurtzite GaN epilayer. Although the XLD spectrum at the Ga K edge presents a contribution from the GaN template, it can be deduced that the (Ga,Mn)N layer preserves the crystallographic symmetry even at a rather high concentration of 6.3% Mn.

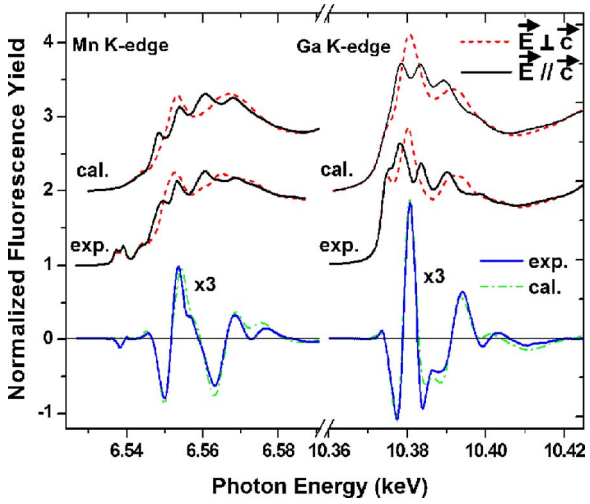

FIG. 3. (Color online) Normalized experimental XANES spectra (shifted by 1) for linearly polarized x-ray light oriented perpendicular and parallel to the c axis and XLD [no shift, blue (dark gray) line] signal recorded at the Mn and Ga K edges for a (Ga,Mn)N epilayer with 6.3% Mn. The calculated normalized convoluted XANES spectra (shifted by 2) are given together with the corresponding calculated XLD spectra [no shift, green (light gray) line].

The XLD spectrum recorded at the Mn K edge (Fig. 3) exhibits very similar spectral shape to the spectrum at the Ga K edge, but with 1.8 times smaller amplitude. In contrast, the XANES spectra at the Mn K edge are quite different from those at the Ga K edge. In particular, we observe two additional peaks at the low-energy side of the absorption edge. These two peaks originate mainly from dipolar $(1s\rightarrow 4p)$ transitions reflecting the Mn impurity $4p$ band hybridized with the $3d$ band located in the GaN gap. The first peak is estimated to contain a small amount (up to 15%) of quadrupolar $(1s\rightarrow 3d)$ transitions.[23] The presence of these two peaks in the XANES spectra indicates that the valence state is mainly Mn^{3+} (d^4) rather than Mn^{2+} (d^5) (where only one peak is observed),[23] as is further confirmed below.

Using the FDMNES code,[24] we have calculated the edge part of the Ga and Mn K-edge XANES and XLD spectra. The simulations were performed using the multiple-scattering formalism within the muffin tin approximation. A $Ga_{15}MnN_{16}$ wurtzite supercell was used, representing a uniformly doped GaN epilayer with 6.25% of Mn. The radius of the cluster was 8.5 Å. The lattice parameters were chosen to be those of bulk GaN. The calculated spectra were convoluted using a Lorentzian function with an energy-dependent

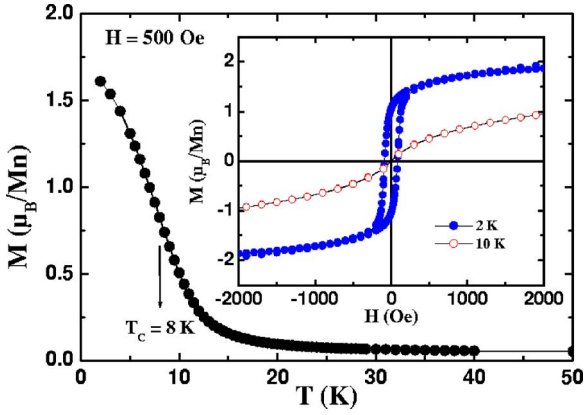

FIG. 4. (Color online) Temperature dependence of the magnetization at a magnetic field of 500 Oe for a sample with 6.3% Mn. The inset shows the magnetization loops at 2 and 10 K for the same sample.

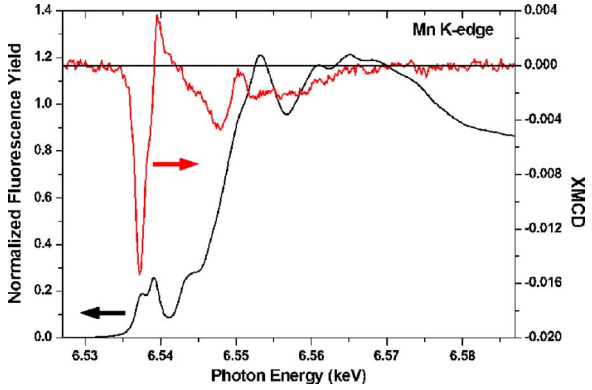

FIG. 5. (Color online) Isotropic XANES spectrum (left scale) and its corresponding XMCD signal (right scale) recorded at the Mn *K* edge measured under 60 kOe in-plane field and at 7 K for a sample with 6.3% Mn.

width, taking into account a core hole lifetime of 1.16 and 1.82 eV for Mn and Ga, respectively. When Mn atoms occupy Ga sites, we observed a very good agreement in spectral shape and amplitude between calculated and experimental XANES and XLD spectra for both Mn and Ga atoms (Fig. 3). For other possible Mn sites occupation, e.g., N-substituted or interstitial sites, no agreement was found with the experimental spectra. Note that if metallic Mn clusters and/or $GaMn_3N$ and/or Mn_4N were present in our sample at a level of 2 at. %, the amplitude of the XLD signal at the Mn *K* edge would decrease at least by 20%, which is easily detectable. Moreover, we observed the same Mn *K*-edge XLD signal (edge part) in shape and in amplitude (within 3%) for all (Ga,Mn)N samples with a Mn concentration ranging from 6.3% down to 0.04%, where the presence of secondary phases is unlikely. In our simulations, the best agreement between calculated and experimental XANES and XLD spectra was obtained for $3d^{4.5}4s^2$ Mn electronic configuration. The XLD experiments show that the Mn atoms are Ga substituted and within the detection limit of the method do not reveal the presence of any secondary phases or metallic clusters, although the presence of an infinitesimal amount cannot be completely excluded.

Magnetization measurements were performed in a 50 kOe superconducting quantum interference device (SQUID) magnetometer, in the temperature range 2–300 K, with the magnetic field applied parallel to the sample surface. To correct the signal from the diamagnetic/paramagnetic contribution of the substrate, identical measurements were performed on a blank substrate of the same shape and dimensions. Figure 4 (inset) illustrates the magnetization loops recorded at 2 and 10 K on (Ga,Mn)N with 6.3% Mn. A clear opening of the hysteresis cycle is observed at 2 K. At 10 K the remanence is no longer observed. The spontaneous magnetization at 2 K $[(2.4\pm0.2)\mu_B$ per Mn] is extracted from the Arrott plot (not shown) of the isothermal magnetization curve given in Fig. 6. The coercive field is $\approx$100 Oe at 2 K whereas the remanent magnetization *M* (2 K,0 Oe) is measured equal to $1.05\mu_B$ reaching only 44% of the spontaneous magnetization. From the thermal variation of the magnetization measured under an applied field of 500 Oe (Fig. 4), we determined, from the maximum in the derivative, a T_C of 8 K. No signature of high-temperature ferromagnetic phases has been observed above 20 K.

To further demonstrate the intrinsic magnetic properties of (Ga,Mn)N, we have performed XMCD measurements at the Mn *K* edge. These experiments were also carried out at the ESRF beamline ID12,[21] using the total fluorescence yield detection mode. The XMCD signal was obtained as a direct difference of two XANES spectra recorded with right and left circularly polarized x rays. A magnetic field was set parallel to the incoming x-ray beam and nearly parallel ($<10°$) to the sample surface. Figure 5 shows the Mn *K*-edge isotropic XANES and XMCD spectra of the $Ga_{0.937}Mn_{0.063}N$ epilayer recorded at 7 K and under an applied field of 60 kOe.

A very intense XMCD signal (1.6% with respect to the edge jump) is observed mainly at the first peak of the XANES spectrum. Since the XMCD signal at the *K* edge is proportional to the orbital polarization of the absorbing atom,[25] our result clearly shows that the Mn atoms in (Ga,Mn)N carry an orbital magnetic moment. This observation is another strong argument in favor of the Mn^{3+} valence state. Indeed, in the case of Mn^{2+} where the 3*d* and 4*p* orbital moments are nearly zero, the XMCD signal is usually one order of magnitude smaller[26] than the signal measured here. Moreover, the negative sign of the XMCD signal suggests that the Mn orbital magnetic moment is antiparallel to the sample magnetization. In (Ga,Mn)As, where the Mn valence state is generally accepted to be +2, the Mn *K*-edge XMCD signal was measured to be positive and 10 times smaller.[27] A free Mn^{2+} ion carries only a spin magnetic moment ($5\mu_B$, $S=5/2$, $L=0$) whereas a Mn^{3+} ion has a spin magnetic moment ($S=2$) and an orbital magnetic moment ($L=2$), antiparallel to the spin, resulting in a total moment of $2\mu_B$. However, the crystal field and the Jahn-Teller effect strongly reduce the orbital moment, resulting in a total magnetic moment between $2\mu_B$ and $4\mu_B$. This is in agreement with our experimental results shown in Fig. 6. This figure shows the temperature-dependent magnetization curves recorded with the SQUID together with the as-measured magnetization

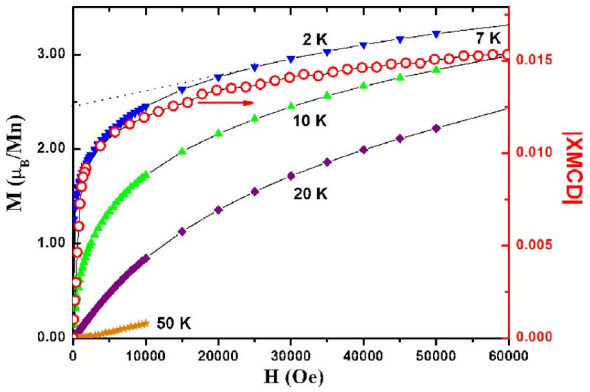

FIG. 6. (Color online) Isothermal magnetization curves for 50, 20, 10, and 2 K measured by the SQUID (full symbols, left scale) and magnetization curve measured at 7 K by monitoring the intensity of the Mn *K*-edge XMCD signal for a sample with 6.3% Mn (open symbols, right scale).

curve recorded by monitoring the Mn *K*-edge XMCD signal as a function of applied field at 7 K. Under high magnetic fields the magnetization of Mn measured via XMCD seems to be saturated while the SQUID data exhibit a rather important slope. This discrepancy might be assigned to the contribution of paramagnetic defects in the sample and/or to errors in the subtraction of the diamagnetic contribution of the substrate since, under high magnetic fields the diamagnetic signal becomes predominant with respect to the ferromagnetic one and the corrected SQUID signal is thus obtained with less accuracy. Under weak magnetic fields, the Mn magnetization measured with XMCD is nearly the same as the total magnetization recorded with the SQUID. This low-field part is a typical signature of a ferromagnetic system.

In conclusion, we have demonstrated that a wurtzite (Ga,Mn)N DMS of high structural quality can be grown by PAMBE. Detailed structural analysis based on x-ray diffraction and x-ray linear dichroism shows that Mn atoms occupy Ga sites with a predominantly +3 valence state. Within the sensitivity of our experimental techniques, no secondary phases were observed. However, although the presence of very small amounts cannot be completely excluded, this does not affect the conclusions drawn from the experimental results. In combination with macroscopic and element-selective magnetic measurements, we determine a spontaneous magnetic moment of $2.4\mu_B$ per Mn at 2 K and a T_C of only 8 K in wurtzite (Ga,Mn)N with 6.3% Mn. This study provides experimental results that unambiguously demonstrate *intrinsic* ferromagnetism in (Ga,Mn)N, which changes completely the present state of research on GaN-based DMSs.

*Corresponding author. Email address: esarig@gmail.com

[1] T. Dietl *et al.*, Science **287**, 1019 (2000).
[2] T. C. Schulthess *et al.*, Nat. Mater. **4**, 838 (2005).
[3] D. J. Keavney, S. H. Chung, S. T. King, M. Weinert, and L. Li, Phys. Rev. Lett. **95**, 257201 (2005).
[4] T. Graf *et al.*, Appl. Phys. Lett. **81**, 5159 (2002).
[5] S. Dhar, O. Branat, A. Trampert, K. J. Friedland, Y. J. Sun, and K. H. Ploog, Phys. Rev. B **67**, 165205 (2003).
[6] S. Sonoda *et al.*, J. Cryst. Growth **237-239**, 1358 (2002).
[7] S. Novikov *et al.*, J. Vac. Sci. Technol. B **23**, 1294 (2005).
[8] K. Sato, W. Schweika, P. H. Sederichs, and H. Katayama, Yoshida, Phys. Rev. B **70**, 201202(R) (2004).
[9] G. Bouzerar, T. Ziman, and J. Kudrnovsky, Europhys. Lett. **69**, 812 (2005).
[10] I. Pop *et al.*, Mater. Chem. Phys. **37**, 52 (1994).
[11] H. Niida *et al.*, J. Appl. Phys. **79**, 5946 (1996).
[12] J. García *et al.*, J. Magn. Magn. Mater. **51**, 365 (1985).
[13] J. Stohr, J. Magn. Magn. Mater. **200**, 470 (1999).
[14] Y. L. Soo *et al.*, Phys. Rev. B **67**, 214401 (2003).
[15] K. W. Edmonds, N. R. S. Farley, T. K. Johal, G. van der Loan, R. P. Campion, B. L. Gallagher, and C. T. Foxon, Phys. Rev. B **71**, 064418 (2005).
[16] P. T. Chiu *et al.*, Appl. Phys. Lett. **86**, 072505 (2005).
[17] P. Stone *et al.*, cond-mat/0604003 (unpublished).
[18] S. Kuroda *et al.*, Appl. Phys. Lett. **83**, 4580 (2003).
[19] R. Giraud *et al.*, Europhys. Lett. **65**, 553 (2004).
[20] C. Brouder, J. Phys.: Condens. Matter **2**, 701 (1990).
[21] A. Rogalev *et al.*, *Magnetism and Synchrotron Radiation* (Springer, Heidelberg, 2001).
[22] J. Goulon *et al.*, J. Synchrotron Radiat. **5**, 232 (1998).
[23] A. Titov *et al.*, Phys. Rev. B **72**, 115209 (2005).
[24] Y. Joly, Phys. Rev. B **63**, 125120 (2001).
[25] H. Ebert, Rep. Prog. Phys. **59**, 1665 (1996).
[26] H. Maruyama, N. Ishimatsu, and N. Kawamura, Physica B **351**, 328 (2004).
[27] T. K. Johal *et al.* (unpublished).